International Journal of Innovative Research in Medical Science (IJIRMS)
Volume 10, Issue 09, September 2025,
https://doi.org/10.23958/ijirms/vol10-i09/2121

Review Article

Quantum Energetics in the Differential Dynamics of Transient mRNA versus Stable DNA

Daniel Santiago, RPh, Pharm D

Independent Researcher, United States.

*Corresponding Author: Daniel Santiago; *sanshou1428@protonmail.com*

Received: 06 August 2025; Accepted: 24 August 2025; Published: 02 September 2025

Abstract

While RNA's 2′ hydroxyl group has long been recognized as a primary contributor to mRNA instability, owing to its heightened susceptibility to hydrolytic cleavage, this manuscript introduces a complementary quantum-biological hypothesis. It explores how vibrational modes, quantum coherence, and electromagnetic coupling influence nucleotide behavior through dynamic, real-time quantized boundary formation, governed by conservation principles such as $E = mc^2$ and $E = hf$.

Crucially, protonation states modulated by pKa transitions amplify local energy fluctuations, fostering transient configurations in mRNA. These instabilities are further shaped by van der Waals (vdW) interactions and the anisotropic nature of three-dimensional molecular geometry, which modulate proximity-dependent quantum effects in a context-sensitive manner. Drawing inspiration from Bohm's implicate order, the study proposes that mRNA's transience reflects a divergent conformational landscape, continuously perturbed by quantum-level variability. In contrast, DNA's relative resilience is attributed to its helical architecture and robust repair mechanisms.

Building on this framework, the manuscript challenges conventional paradigms by advancing a quantum-biological model to explain both the inherent instability of natural mRNA and the enhanced stability of its N1-methylpseudouridine (m1Ψ)-modified variant. It reconceptualizes nucleotide resilience through the lens of vibrational dynamics, quantum coherence, and electromagnetic interactions, integrated with classical physical principles.

The study further investigates how m1Ψ influences polarity, folding, and base stacking in therapeutic mRNA. Although structurally analogous to thymidine in DNA rather than uridine, m1Ψ does not achieve full energetic equivalence. The central hypothesis, bridging quantum physics and molecular biology, is that m1Ψ must confer stabilizing effects comparable to thymidine, mitigating quantum-scale fluctuations through emergent structural coherence.

The pivotal question remains: is N1-methylpseudouridine a functionally equivalent substitute for uridine in therapeutic contexts?

Keywords: ***Quantum Biology, mRNA Stability, Nucleic Acid, Vibrational Modes, Nucleotide, Nucleoside, Energy States***

Introduction

Messenger RNA (mRNA) and DNA both encode genetic information but differ significantly in structural stability. The rapid degradation of mRNA is typically attributed to its 2′ hydroxyl group, which promotes phosphodiester bond hydrolysis [1,2]. DNA, lacking this group, benefits from a double-helix structure and repair systems that enhance its resilience [2,3]. Yet classical biochemistry cannot fully express the energetic complexity governing nucleic acid behavior.

The perspective introduced here proposes that mRNA and DNA occupy distinct quantum energy landscapes, shaped by emerging principles in quantum biology (**Table 1**) [4,5].

Coherence, tunneling, and electromagnetic coupling are not merely quantum abstractions; they are materially modulated by biophysical variables such as pKa, van der Waals forces, and conformational geometry. Protonation states, governed by pKa, which quantifies an acid's propensity to donate a proton, influence electromagnetic fields and hydrogen-bonding networks, thereby modulating tunneling probabilities and decoherence thresholds. Van der Waals interactions, weak non-covalent forces arising from transient dipoles induced by temporary distortions of electron clouds, contribute to base stacking and spatial dispersion, shaping resonance stability and electron-cloud behavior.

The three-dimensional architecture of nucleic acids regulates dipole orientation and accessibility to quantum vacuum fluctuations, critically impacting coupling efficiency and the topology of the energy landscape. Building on Bohm's implicate order, where matter emerges from condensed vibratory energy, this hypothesis explores biological emergence as a continuum of uninterrupted energy flux. It shows the connection between quantum-level repulsion (e.g., Pauli exclusion) with macroscale energy transformations such as photosynthesis [6,7].

Drawing on Peirce's proofs of molecular interpenetration and atomic exclusion [8], the perspective proposed here proposes that mRNA's transience arises from destabilizing quantum fluctuations and vibrational interactions. In contrast, DNA's durability may stem from coherent energy configurations stabilized by structured water layers [9] and ultra-weak photon emissions (entropy) [10]. Modified nucleosides, including N1-methylpseudouridine (m1Ψ) in

therapeutic mRNA, are examined through this quantum-biological lens [11], with implications for translational stability and molecular resilience. The interplay between pKa transitions, anisotropic geometries, and quantum-boundary dynamics enables something like an emerging multidimensional map of nucleotides as they come into existence by construction.

Literature Review

Growing evidence in quantum biology reveals significant quantum effects in nucleic acid vibration and stability. Table 1 compiles research on coherence, tunneling, and vibrational interactions that influence genetic processes and cellular signaling [3,7,10,12-15]. Spectroscopic analyses show hydration-dependent backbone differences linked to RNA's 2′ hydroxyl group [16-18]. DFT modeling, including Jiang (2020) [19], highlights nucleobase dynamics, while findings on underdamped phonon-like modes [13], anharmonic delocalization [20], and scaled quantum fields [21] suggest that DNA's durability and mRNA's transience emerge from quantum vibrational encoding that cannot be accounted for within the large-scale principles of classical biochemistry.

Theoretical Framework: Quantum Dynamics in Nucleic Acids

At the molecular scale, quantum processes govern the behavior of nucleic acids. Two key phenomena, vibrational modes and quantum coherence, play critical roles in shaping mRNA and DNA.

Vibrational Modes

Vibrational modes are rhythmic atomic oscillations within a molecule [14].

- In RNA, the 2′ hydroxyl group facilitates intramolecular hydrolysis, which increases degradation susceptibility [2,16,18].
- Chemical modifications such as m1Ψ enhance stability by increasing the mass of the nucleoside, analogous to adding heavy steel to a bridge to better resist wind loads [4,11,14,22-25].

Quantum Coherence

Quantum coherence involves maintenance of fixed phase relationships across quantum states, allowing synchronized energy distributions among subunits in biological systems [5,7,26].

- In DNA, vibrational energy distributions may contribute to structural stability, potentially influenced by quantum effects such as proton tunneling [13,26,27].
- Quantum effects, such as proton tunneling, influence DNA stability and replication, interacting with classical processes like enzymatic activity [3,12,15,26,27].

Mathematical Modeling: Open Quantum Systems

The Lindblad master equation, a general form of Markovian master equations, provides a framework for modeling quantum behavior in open systems at the atomic and molecular scales by incorporating environmental decoherence, potentially applicable to nucleic acids [28,29]. Lindblad approach extends Schrödinger's equation to accommodate system environmental interactions.

$$\frac{d}{dt}\rho = -i[H,\rho] + \sum_k \Gamma_k \left(L_k \rho L_k^\dagger - \frac{1}{2}\{L_k^\dagger L_k, \rho\} \right)$$

- The Hamiltonian (H) in the Lindblad equation includes harmonic oscillator terms, relevant to modeling systems like nucleobases [14,19,28,29].
- The Lindblad modification accounts for environmental noise, capturing system environment interactions [28,29].

Table 1: Spectral Signatures and Quantum Dynamics in Nucleic Acids

Research Demonstrating Quantum Effects at the Scale of Atoms and Molecules in Nucleic Acids	Reference
Vibrational Modes in DNA/RNA: Attenuated Total Reflectance (ATR–FTIR) spectroscopy of nucleobases progresses toward oligonucleotides and full strands, revealing hydration dependent vibrational behavior. Quantum chemical modeling predicts spectral frequency and intensity.	Heidari (2016) [17]
Quantum Coherence in DNA Structures: Underdamped phonon-like modes observed in G-quadruplexes and B-DNA suggest quantum coherence as a stabilizing factor in nucleic acid architectures.	González-Jiménez, M., Ramakrishnan (2021) [13]
Theoretical Modeling of Vibrational Spectroscopy: Density functional theory (DFT) simulations forecast vibrational couplings in nucleobases, linking theoretical predictions with experimental spectra and providing atomistic insights into molecular dynamics	Jiang, Y., & Wang, L. (2020). [19]
Anharmonic Vibrational Coupling: 2D IR spectroscopy identifies delocalized vibrational modes spanning purine and pyrimidine rings, consistent with quantum delocalization in base structures.	Peng, C. S., Jones, K. C., & Tokmakoff (2011) [20]
Quantum Mechanical Force Fields: Neutron scattering and scaled force field analysis uncover vibrational dynamics in pyrimidine bases (uracil, thymine, cytosine), indicating potential stability encoding mechanisms.	Aamouche, A., Ghomi, M., Letellier, R., Liquier, J., Morvan, F., Cadet, J., & Taillandier, E. (1995) [21]

- Quantum coherence in biological systems, such as in photosynthetic energy transfer, may be sustained under environmental stress through efficient energy transfer systems [5,7].

Mass-Energy Equivalence and Molecular Modifications

Modifying uridine to m1Ψ adds approximately 14.03 Daltons of mass, subtly shifting its UV absorption spectrum and dampening certain vibrational modes, a reflection of altered electronic and steric interactions within the nucleoside [11,14,22,24]. Studies link m1Ψ incorporation to enhanced mRNA stability, improved translational efficiency, and reduced immunogenicity [23,31,32,36,38,46].

While Einstein's equation ($E = mc^2$), is most evident as manifested in high-energy physics, it underscores the fundamental interchangeability of mass and energy. Energy, mass, and light arise from the same quantum-relativistic substrate: photons can generate matter, and matter can return to light, as observed in electron-positron annihilation in the Breit-Wheeler process [39]. The energy equivalent of $\Delta m \approx 14$ Da is considered negligible relative to the thermal and chemical energies in biological systems. Therefore, mRNA physicochemical behavior is governed primarily by

modifications to hydrogen bonding networks, base stacking, and solvent interactions, rather than by any measurable relativistic conversion [18,34,36].

In the context of mRNA therapeutics, even minute mass and structural changes can alter local folding dynamics and enzymatic activity, thus affecting half-life and interaction profiles [40-42]. These combined effects illustrate how quantum level modifications to nucleotide mass propagate through classical molecular dynamics to influence therapeutic performance.

Quantum-Level Alterations in RNA Therapeutics

Quantum changes in nucleic acids, such as electron redistribution, dipole moment shifts, influence molecular properties like hydrogen bonding, base stacking, and solvation energetics, shaping RNA behavior [2,5,14,19]. These properties affect vibrational dynamics, electrostatic interactions, and chemical reactivity, which can be modeled using quantum mechanical approaches like density functional theory (DFT) [14,19,52]. Density Functional Theory (DFT) is a quantum mechanical method that calculates the electronic structure of atoms, molecules, and solids by modeling electron density rather than wavefunctions.

Modifications in RNA nucleotides, such as pseudouridine and N1-methylpseudouridine, lead to biological effects (**see Table 2**):

- **Solvation energetics:** Influencing hydration shells and solvent interactions, impacting RNA stability [9,18,24]
- **Hydrogen bonding capacity:** Changes in donor-acceptor geometries, RNA secondary structure [34,36,47]
- **Electrostatic potential:** Shifts in charge distribution and pKa shifts affect molecular interactions [24,52]
- **Van der Waals forces:** Noncovalent interactions are modulated, influencing base stacking [19,47,54]

These effects are exemplified by pseudouridine (Ψ) and N1-methylpseudouridine (m1Ψ). The C-glycosidic bond in Ψ redistributes electron density without changing molecular mass (**see Figures 1,2, and 3**), strengthening stacking interactions and hydrogen-bonding [34,36,47,11]. Substituting m1Ψ for the canonical uridine increases molecular mass (~14 Da), introducing nonpolar perturbations that reshape dipolar interactions and vibrational spectra [11,14,24].

Table 2: Quantum-Level Effects of RNA Base Modifications

Feature Altered	Molecular Impact	Biological Consequence
Electron density redistribution	Changes in dipole moments and polarizability	Alters solvation, bonding, and pKa behavior (Table3)
Orbital configuration	Modulation of hydrogen bonding and stacking angles	RNA secondary structure
N1-methylation in m1Ψ	Adds nonpolar bulk, shifts electron cloud dispersion	Affects van der Waals interactions and resonance (Table 4)
Dipolar reorientation (dehydration)	Elevated dipole moments, increased H-bond donation	Electrostatic affinity and folding dynamics
Vibrational coupling	Alters IR/Raman spectra and flexibility	Reveals quantum-coherent modulation of base stacking

These modifications enhance mRNA stability, translational efficiency, and reduce immunogenicity [22,23,31,32,46]. In mRNA therapeutics, such changes influence folding dynamics, enzymatic recognition, and therapeutics persistence, bridging quantum level alterations to classical molecular outcomes [22,40,46].

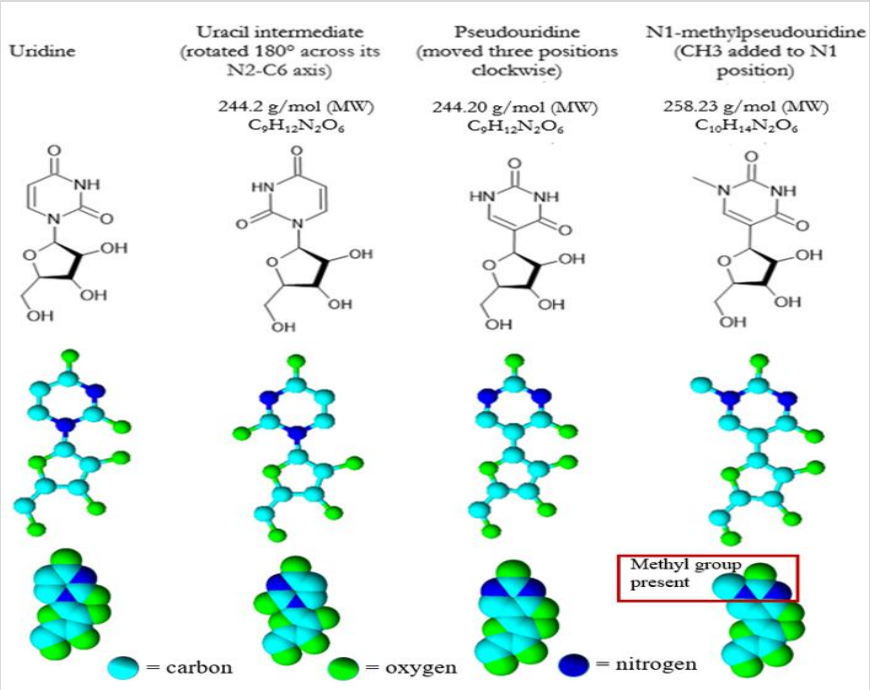

Figure 1: The series of chemical diagrams given here, from [11], shows the transformation from uridine to m1Ψ: the top row shows the traditional flat (two dimensional textbook chemical diagrams); the second row shows the three-dimensional ball-and-stick models; and the third row shows the three-dimensional van der Waals distance-dependent force interaction spaces theoretically occupied by the atoms involved. In the colored diagrams, aqua represents carbon; green, oxygen; and dark blue, nitrogen. The parts that are changing as the progression takes place from uracil to m1Ψ are shown left to right across the page. Sources: PubChem, Uridine C9H12N2O6, CID 6029; Pseudouridine, C9H12N2O6, CID 15047; ACS, m1Ψ - American Chemical Society (acs.org). Drawn by the author with Molview.com and ChemSketch programs.

Integrating Quantum-Derived Electron Distributions with pKa-Driven Behavior

By integrating quantum-derived electron distributions with pKa-driven chemical behavior, we can more accurately predict acid–base equilibria and reactivity in nucleic acids [5,14,19,52,54].

Why pKa Matters for Thymine (5-methyluracil) and Uracil

1. Base pairing and hydrogen bonding:

A. pKa controls protonation states at N3 (uridine) or N3/N1 (pseudouridine), tuning hydrogen-bond donors and acceptors in A–T versus A–U pairs [34,52,74]. (**see Table 3**);
B. Tautomerism is involved [5,52];
C. Shifts in pKa influence the equilibrium between keto and enol tautomers [5,52];
D. Chemical stability and reactivity come into play [34,52];
E. A higher pKa makes a base less prone to acid-catalyzed deamination or ring opening, affecting long-term integrity [2,52]; and
F. the specificity of DNA vs. RNA Specificity must be considered [2,50].

2. The 5-methyl group of thymine elevates its pKa above that of uracil (**Table 3**), rendering it marginally less acidic and more chemically stable, these being traits well suited for DNA's archival function. In contrast, the lower pKa of uracil aligns with RNA dynamics [2,52].

Role of pKa in Nucleoside Behavior and RNA Dynamics

The acid dissociation constant (pKa) of a nucleoside dictates its protonation state under physiological pH, directly impacting its hydrogen bonding, stacking interactions, and overall chemical reactivity [2,34,36,52,74].

Because nucleosides consist solely of a nitrogenous base and a sugar, their pKa values reflect only the ionizable groups on those moieties, whereas nucleotides, which also include one or more phosphate groups, exhibit additional, characteristic phosphate-group dissociations in their pKa profiles alongside the base and sugar functionalities [2,18,52].

Key implications of pKa in RNA systems:

- Protonation influences base-pairing fidelity and local backbone conformation [2,34,52]
- Shifts in pKa from quantum-level modifications alter electrostatic profiles and solvation shells [5,9,24,52]
- Combined with alterations in dipole moment and polarizability, pKa shifts must affect molecular energetics impacting stability [14,19,24,52]

By integrating quantum-derived electron distributions with pKa-driven chemical behavior, the processes by which modified nucleotides calibrate RNA folding and function begin to appear [5,24,47,52].

Molecular Weight Perspective

We currently lack empirical pKa data for m1Ψ (**Table 3**); however, the extra methyl substituent is expected to perturb the nucleotide acid-base profile [11,24,53]. Determining the pKa of m1Ψ is therefore crucial for understanding how this modification modulates RNA stability and fidelity.

Although pKa and molecular weight (MW) are distinct physicochemical parameters, they interact to shape a molecule's behavior across physical, chemical, and biological contexts. Changes in MW do not inherently alter pKa, unless substituents shift electron density, as seen in Figure 3, but together, these descriptors govern interactions within the environment, from phase transitions and vibrational spectra to biopharmaceutical performance. Consequently, both pKa and MW are indispensable molecular descriptors [11,14,19,24,52].

In biopolymers such as DNA and RNA, higher MW generally correlates with increased mechanical strength and chemical resistance at the cost of reduced processability. Lower-MW polymers flow more easily yet sacrifice structural resilience [2,48,49]. Think of RNA as a long necklace of repeating beads (nucleotides); longer chains tangle more, enhancing toughness while impeding flow, much like synthetic polymers do. In cells, ribosomal RNA (rRNA) synthesized in the nucleolus forms entangled, gel-like networks that scaffold ribosome assembly and maintain nucleolar integrity. Its molecular weight drives these viscoelastic properties, as longer chains (higher MW) promote gel-like behavior, while shorter, folded subunits (lower MW) facilitate mobility [48,49].

That increase in MW comes at a cost: longer RNA strands fold more slowly, are harder to transport, and face processing delays due to size and entanglement [25,48,49]. By contrast, shorter RNAs are more flexible, easier to isolate, and can move freely through cellular compartments, but they may lack the structural resilience for complex functions, much like lightweight plastics that snap under stress.

At the codon level, substituting uridine (U, 112.09 g/mol) with N1-methylpseudouridine (m1Ψ, 258.23 g/mol) introduces an approximate mass increase of 14.03 g/mol per nucleoside per codon. This cumulative shift elevates the overall molecular weight of mRNA, particularly in codons containing uridine, as detailed in Table 2 of Santiago (2024) [11]. The increase affects the molecule's viscosity and intramolecular interactions in both in vitro and in vivo contexts [11,48,49,53]. Table 4, which presents the van der Waals initiation sequence, illustrates the conformational change observed in the AUG codon. Similar structural alterations occur in every codon where uridine is replaced by m1Ψ.

Table 3. Measured pKa Values of Key Nucleosides

	Uracil ($C_4H_4N_2O_2$) RNA	**Uridine ($C_9H_{12}N_2O_6$) RNA**	**Pseudouridine ($C_9H_{12}N_2O_6$) RNA**	**Thymine ($C_5H_6N_2O_2$) DNA/RNA [50]**	**Thymidine ($C_{10}H_{14}N_2O_5$) DNA**	**m1Ψ ($C_{10}H_{14}N_2O_6$) RNA**
pka (Measured position)*	9.45	9.25 (N3)	9.1 (N1) 9.6 (N3)	9.9	9.8	Not explicitly listed in available sources.
Van der Waals value † (vdW;Å³/molecule) [51]	125	195.46	195.46	148	203.97	212.76
Molecular Weight (g/mol)*	112.09	244.20	244.20	126.11	242.23 (if RNA 258.23, $C_{10}H_{14}N_2O_6$)	258.23

** Jones, E. L., Mlotkowski, A. J., Hebert, S. P., Schlegel, H. B., & Chow, C. S. (2022) [52] and PubChem (2025) [53]; † Values based on Bondi radii, excluding conformational details or solvent effects on intrinsic molecular volume. Note: The van der Waals volume estimation method is detailed in the Notes section and reflects intrinsic molecular volume [51]. Van der Waals interactions underpin a broad spectrum of physical and chemical behaviors in matter [54].*

Although N1-methylpseudouridine is supposedly derived from pseudouridine, its physicochemical properties, particularly its molecular weight and methylation pattern, more closely resemble those of thymidine than pseudouridine. Notably, thymine (**126.11 g/mol**) is typically absent from RNA, with transfer RNA (tRNA) representing a key exception [50,53]. Its molecular weight closely resembles that of N1-methylpseudouracil (**126.12 g/mol**), which corresponds to pseudouracil (112.09 g/mol) plus a methyl group (14.03 g/mol). If thymine is conjugated with a ribose moiety, adding an additional oxygen atom (16 g/mol), the resulting nucleoside mass increases to **258.23 g/mol**, identical to that of N1-methylpseudouridine (**258.23 g/mol**), as shown in Table 3. In nucleosides, the ribose is covalently bonded to the base, often with stereochemical modifications that impact its overall mass and functional behavior.

This polymer analogy underscores how universal physical principles, like chain entanglement, govern RNA behavior, from ribosome biogenesis in cells to RNA based techniques in research. Molecular weight isn't just a number; it's a fundamental determinant of RNA's biological roles.

A Unified View of Quantum Perturbations and Van der Waals Forces

N1-Methypseudouridine (Table 4)

Compared to pseudouridine (Ψ), N1-methylpseudouridine introduces enhanced steric bulk and altered charge from its methyl group [11,23]. These shifts manifest across multiple molecular dimensions:

- Methyl substitution in N1-methylpseudouridne reshapes electronic structure and hydrogen placement, potentially influencing tautomeric dynamics (**see Figure 1,2, and 3**).
- Reconfigured RNA architecture: folding landscapes shift, impacting geometry and folding patterns [23,34,46,47] (**see Table 4**).
- Immune invisibility: m1Ψ reduces recognition by Toll-like receptors (TLR) and retinoic acid-inducible gene I (RIG-I), dampening innate immune activation [23,31,32,55].

These adaptations boost translational efficiency [23,46] (**see Table 5**), but carry risks:

- increased frameshifting [38],
- suppressed interferon signaling [23,38,55], and
- m1Ψ may induce IgG4 class switching [41,42].

Quantum-level effects, such as electron redistribution and dipolar shifts in modified nucleotides, do influence molecular interactions at the atomic and macromolecular scales, extending to cellular processes like RNA folding and immune responses, underscoring the need for multiscale modeling frameworks that integrate quantum physics with molecular biology, and immunology.

Van der Waals Forces and Base Stacking

Van der Waals (vdW) forces arise from transient dipoles induced by fluctuating electron clouds. Although individually weak, these interactions become collectively significant in large biomolecules and undergird key aspects of nucleic acid structure and function [2,19,54]. While pKa-driven hydrogen bonds dictate specific base pairing, vdW forces govern base stacking, backbone packing, and the fine-tuning of molecular conformation [34,36,52,54].

- Additivity in assemblies: Thousands of vdW contacts in an RNA duplex or ribosome-mRNA complex yield substantial stabilization [2,48,54].
- Synergy with pKa: Protonation states establish hydrogen-bond networks that align bases; vdW forces then lock them into quantized and optimal stacking geometries [5,14,52,74].
- Aromatic ring stacking: Planar rings of uracil, thymine, and modified bases maximize π-π contacts. Methylation in m1Ψ increases vdW volume (~195 Å³ → ~213 Å³, **Table 3**), enhancing stacking and modulating helix rigidity [11,34,36,47,51].

Integrating van der Waals interactions with quantum-derived electron distributions and pKa profiles provides a framework for understanding how molecular perturbations influence RNA folding, stability and 3D architecture [14,19,47,52,54].

Structural Comparisons of Uridine and m1Ψ

The substitution of uridine (U) by N1-methylpseudouridine (m1Ψ) in synthetic (therapeutic) mRNA, especially in COVID-19 vaccines, imparts unique structural and energetic properties [11,23,38]. Although m1Ψ shares geometric similarities with thymidine, most notably in its comparatively closer van der Waals volumes (**see Table 3 & 4**), its unique nitrogen positioning and N1 methylation redistribute electron density and reshape local polarity [4,11,23,38,50]. (**see Figure 3**)

At the quantum-level, these modifications influence RNA behavior through [11,23,38,47]:

- base-pairing energetics, which modulate ribosomal decoding fidelity and wobble codon recognition,
- hydrogen bonding geometry,
- dipole moment and charge distribution as well as,
- stacking interactions.

Structural analyses reveal that substituting N1-methylpseudouridine for uridine in mRNA changes molecular conformation (**see Table 4**), thereby affecting stereochemistry and ribosomal interactions [11,23,47]. Van der Waals volume estimates (**Table 3**) show that thymidine (203.97 Å³) and m1Ψ (212.76 Å³) are significantly larger than uridine (195.46 Å³) and pseudouridine (195.46 Å³), reflecting their enhanced steric profiles. Table 3 also highlights pKa values, which govern base-pairing dynamics and protonation behavior. While uridine and pseudouridine exhibit pKa values near 9.25 to 9.6 (N3), thymidine trends higher (~9.8), and m1Ψ more closely resembles to thymidine. These shifts suggest that m1Ψ substitution alters mass and volume and also modulates electrostatic and hydrogen-bonding interactions crucial to ribosomal decoding and mRNA stability.

Although m1Ψ is intended to preserve the encoded amino acid sequence, it does affect spike protein translation and immunogenicity by modifying RNA folding and ribosomal decoding fidelity [11,23,38,41,42,56]. These findings reinforce the principle that biological function emerges from precise three-dimensional conformation and electronic configuration [2,47,57].

Electronic Transitions and UV Absorption

N1-methylpseudouridine exhibits a red-shifted UV absorption maximum (λmax = 272 nm) compared to uridine (λmax = 262 nm), along with a 39.8 % decrease in absorbance at 260 nm [24]. For context, thymidine absorbs maximally at 267 nm. These spectral shifts reflect altered electronic transitions that can influence mRNA secondary-structure formation, and downstream translation efficiency and immune recognition [14,22,23,24,31,32].

Relativistic Considerations in Molecular Excitations

Einstein's mass–energy equivalence ($E = mc^2$) encapsulates the fundamental interchangeability of mass and energy. In molecular UV excitations, unlike in nuclear reactions, no measurable mass-energy conversion takes place [39]. Instead, relativistic corrections subtly shift orbital energy levels, an effect that grows with atomic number and is essentially accepted as negligible in light-atom biomolecules. Even so, specialized systems such as photosynthetic complexes, exploit quantum coherence and wavelike energy transfer, illustrating how even minute relativistic contributions can help shape biological function [7,58].

Ultimately, $E = mc^2$ acts not as a driver of dramatic mass to energy transmutation, but as a foundational constraint on light-matter interactions, subtly tuning molecular dynamics through the architecture of physical law [7,58]. This perspective reinforces the Nobel-recognized principle that biological outcomes hinge on molecular shape and electronic distribution. Accordingly, the energetic landscapes defined by electron redistribution across polar domains differ markedly between uridine and N1-methylpseudouridine (**see Tables 2-4, Figure 3**) [11,23,24,57].

Hypothesis for Nucleotide Behavior

This hypothesis explores biological emergence through quantum and classical interactions in nucleotides. Within a unified quantum-classical framework, nucleotides occupy discrete vibrational energy levels and undergo proton or electron tunneling, modulating chemical reactivity and structural stability [13,16,19,20,26,59]. Temporal coherence, defined as the duration over which wave-like phases remain predictable, influences molecular dynamics, potentially affecting base pairing interactions [5,7,62]. Density functional theory (DFT) and vibrational spectroscopy reveal how quantized vibrational modes and hydration conditions shape classical bonding networks in RNA [9,13,14,19,20,52,63].

In mRNA, the 2'-hydroxyl group contributes to phosphodiester bond cleavage susceptibility, while N1-methylpseudouridine (m1Ψ) methylation alters vibrational frequencies, enhancing backbone stability against hydrolysis [18,22,23,31,47]. Hydration-sensitive vibrational modes influence mRNA folding and ribosomal interactions, whereas DNA leverages excitonic coupling in stacked bases to maintain duplex stability. G-quadruplex structures exhibit vibrational resonances that may support structural integrity [13,16,26,59,61].

Future Directions

1. Quantify vibrational and electronic perturbations using DFT calculations and vibrational spectroscopy to analyze m1Ψ's effects on RNA stability [14,19,52].
2. Correlate UV spectral shifts with real-time folding assays to study mRNA conformational dynamics during translation [24,40].
3. Model m1Ψ's electrostatic profile to assess impacts on intracellular stability and immune recognition, integrating molecular dynamics and immunogenicity data [23,31,41,42].
4. Explore codon optimization strategies to balance translation fidelity and folding kinetics using bioinformatics [46].
5. Investigate hydration and ionic effects on vibrational dynamics in nucleic acids via time-resolved spectroscopy [9,62,63].

Table 4. In the colored diagrams, aqua represents carbon; green, oxygen; maroon, phosphate; and dark blue, nitrogen. The rows of this table show the chemical structures of uridine, pseudouridine, N1-methylpseudouridine, 5-methyluracil (thymine, thymidine). Rows display Van der Waals dynamic stereoscopic shapes of each structure, respectively. AUG is the initiation codon in mRNA that signals the start of protein synthesis during translation in cells. Thymine is typically absent in RNA; however, the exception is transfer RNA (tRNA) [50]. Drawn by the author with ChemSketch.

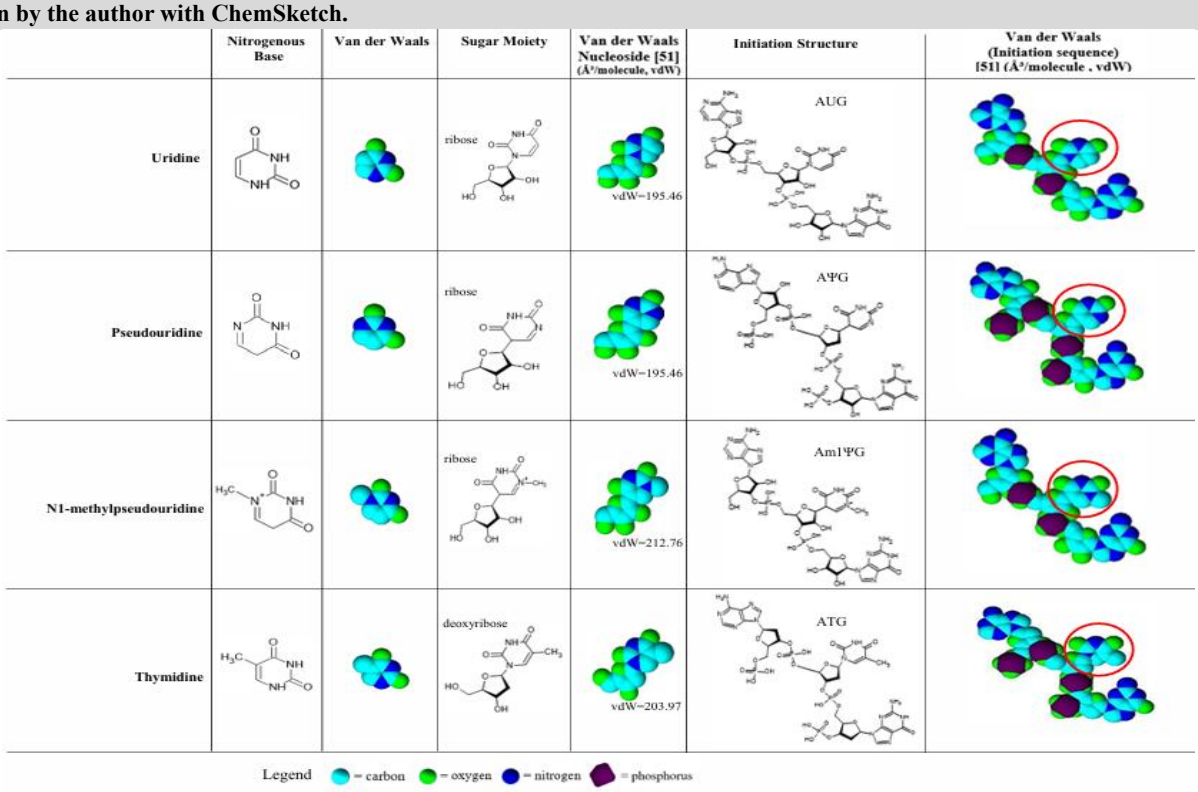

Proposed Methods

Quantum-level influences on nucleic acid dynamics can be investigated by the following interdisciplinary methods:

1. Vibrational spectroscopy

Use Raman and infrared (IR) spectroscopy to profile the vibrational energy states in both native and chemically modified forms of mRNA and DNA. Particular attention should be paid to N1-methylpseudouridine variants, which display distinct spectral shifts. Finol (2024) reported a λmax transition from uridine (262 nm) to pseudouridine (263 nm), to thymidine (267 nm) and to N1-methylpseudouridine (272 nm) [24]. These shifts are associated with enhanced molecular stability, reduced immunogenicity, and elevated protein expression (**see Table 5**), underscoring the need for systematic validation [23,65,47,34,66,67].

Integrating vibrational spectroscopy with quantum dynamic analysis may unveil nuanced interactions between chemical modification and quantum behavior in nucleic acid degradation [17,20,35].

2. Electromagnetic Field Interaction Studies

Investigate the influence of electromagnetic fields (EMF) on nucleic acid vibrational and electronic dynamics by applying controlled frequencies to in vitro mRNA and DNA samples. Experiments will assess changes in vibrational spectra or stability, building on evidence that EMF can perturb molecular interactions in biological systems [63,68,69,70]. m1Ψ's altered vibrational frequencies and enhanced stability suggest potential sensitivity to EMF, warranting studies to explore frequency-dependent effects on molecular dynamics [16,24].

3. Quantum Vacuum Simulations

Leverage DFT and quantum field approximations to simulate the influence of vacuum fluctuations and zero-point energy on nucleotide behavior. Approaches such as Density functional theory (DFT) and quantum field approximations can offer insight into potential energetic contributions to molecular stability, particularly in contexts that elude classical explanations [14,19,52].

4. Endogenous electromagnetic and Photon Emission Analysis

Measure ultra-weak photon emissions from nucleic acids using high-sensitivity photodetectors to probe molecular configuration and dynamics. Such emissions, observed in DNA, may correlate with electronic or vibrational states, providing insights into quantum-biological pathways affecting nucleic acid stability [10,64]. These measurements aim to characterize potential links between photon emission patterns and molecular behavior.

Together, these methods aim to generate experimental and computational evidence for quantum-biological influences alongside classical biochemical models. This integrative approach holds promise for advancing our understanding of genetic material's energetic architecture and expanding the toolkit of molecular biology [10,14,17,20,24,35,52,63,64,68-70].

Discussion

mRNA versus DNA behavior in Therapeutic Contexts

Synthetic mRNA incorporating N1-methylpseudouridine (m1Ψ) demonstrates enhanced protein expression, reduced innate immune activation, and prolonged tissue persistence compared to unmodified RNA [22,23,31,32,40]. These advantages arise from classical biochemical effects, dampened hydrolysis via 2′-OH modulation, and quantum phenomena that subtly tune molecular dynamics.

Challenges and Empirical Pathways

Quantum coherence in nucleic acids remains largely theoretical, with structural stability and ionic shielding recognized as predominant factors. Detecting femtosecond–picosecond coherence or tunneling requires advanced techniques [2,7,13,16,59,12,15]:

- advanced vibrational spectroscopy (FTIR, Raman),
- computational modeling (DFT, quantum molecular dynamics) to predict excitonic coupling and mode lifetimes, and
- correlation of spectroscopic signatures with biophysical markers.

Addressing Skepticism

Quantum effects complement rather than replace classical systems and principles. Notable examples include:

- energy transfer efficiency in photosynthetic complexes via coherence [7,58],
- proton tunneling lowering activation barriers in enzyme-catalyzed DNA repair [12,15,59,70], and
- underdamped vibrational modes in G-quadruplexes enhancing nuclease resistance [13,61].

The foregoing processes illustrate how non-classical forces can synergize with familiar biochemical pathways [3,16,71,47].

m1Ψ as a Thymidine Analog

Comparative data indicate that m1Ψ's UV absorption (λ_max = 272 nm), van der Waals volume (212.76 Å³), and three-dimensional geometry resemble thymidine more than uridine. These characteristics suggest a similarity to DNA-like stability within RNA constructs (**Figure 2, Table 4**) [24]. Such thymidine-like behavior enhances base stacking, reduces hydrolytic degradation, and improves translational fidelity, properties central to prevailing modified mRNA therapeutic optimization theories [11,22,31,32,47,34,36].

Understanding the interplay among molecular pKa, van der Waals volume, and electronegativity is essential, as these parameters govern structural resilience and electron distribution in chemical and biological systems [2,51,52].

Bondi Radii

The Bondi radii, introduced by A. Bondi in 1964 and expressed in ångströms (Å), quantify atomic size in non-bonded interactions by measuring the distance from the atom's nucleus to the outer boundary of its electron cloud, where van der Waals forces dominate [72,73,74]. These radii generally decrease across a period as electronegativity increases, because a greater effective nuclear charge pulls electrons inward, reducing the effective atomic volume. Figure 2 continues the data presented in Table 4.

Table 5. Evidence from Already Published Research Studies

Proposal	Effect	Conclusion	Reference
m1Ψ-modified mRNA	-mRNAs containing the N1-methylpseudouridine (m1Ψ) modification alone and/or in combination with 5-methylcytidine (m5C) outperformed the current state-of-the-art pseudouridine (Ψ) and/or m5C/Ψ-modified mRNA platform by providing up to ~44-fold (when comparing	Enhanced: -Protein Expression -Translational Lifetime and Duration of Expression	Andries 2015 [31]

	double modified mRNAs) or ~13-fold (when comparing single modified mRNAs) higher reporter gene expression upon transfection into cell lines or mice, respectively. - (m5C/)m1Ψ-modified mRNA showed lower intracellular innate immunogenicity and better cellular viability than (m5C/)Ψ-modified mRNA in vitro.	-Reduced Immunogenicity	
m1Ψ substitution enhances the performance of synthetic mRNA switches in cells	-The observed phenomena stem from the high protein expression from m1Ψ containing mRNA -Efficient translational repression in the presence of target microRNAs or proteins. -Synthetic gene circuits with m1Ψ significantly improve performance in cells.	-Observations revealed that m1Ψ enables better fold-change between ON and OFF states of mRNA switches due to the increased basal protein expression at ON state -Stronger m1Ψ-A base-pairing and the lowered innate immune response	Parr 2020 [22]
m1Ψ modification correlates with protein expression, immunogenicity, and stability of mRNA.	-Compared to high-ratio m1Ψ modification, such as 50%, 75%and 100%, low-ratio m1Ψ modification exhibited higher protein translation efficiency. -The relationship between protein expression level/duration and immunogenicity/stability is not linear. -The limitation of this study is that only one mRNA sequence was used	-Findings indicate that m1Ψ modification effectively reduces mRNA immunogenicity and enhances its stability, with a positive correction observed between modification ratio and stability.	Chen 2024 [32]
Deep learning model that predicts mRNA degradation at **nucleotide-level resolution**	-The model outperforms previous approaches (e.g., DegScore, RNA folding algorithms) in predicting **degradation properties**, a major factor in mRNA instability. -It shows **strong correlation with in vitro half-life data**, making it a valuable tool for designing more stable mRNA sequences.	May support claim that m1Ψ reduces hydrolysis rates and enhances mRNA stability.	He 2023 [40]

The relationship between Bondi radii (van der Waals radii) and electronegativity is not a simple linear correlation. Instead, both properties reflect how nuclear charge and electron configuration shape atomic size and bonding behavior. Bondi radii describes the distance at which nonbonded atoms interact without forming a chemical bond, while electronegativity measures how strongly an atom attracts electrons within a bond.

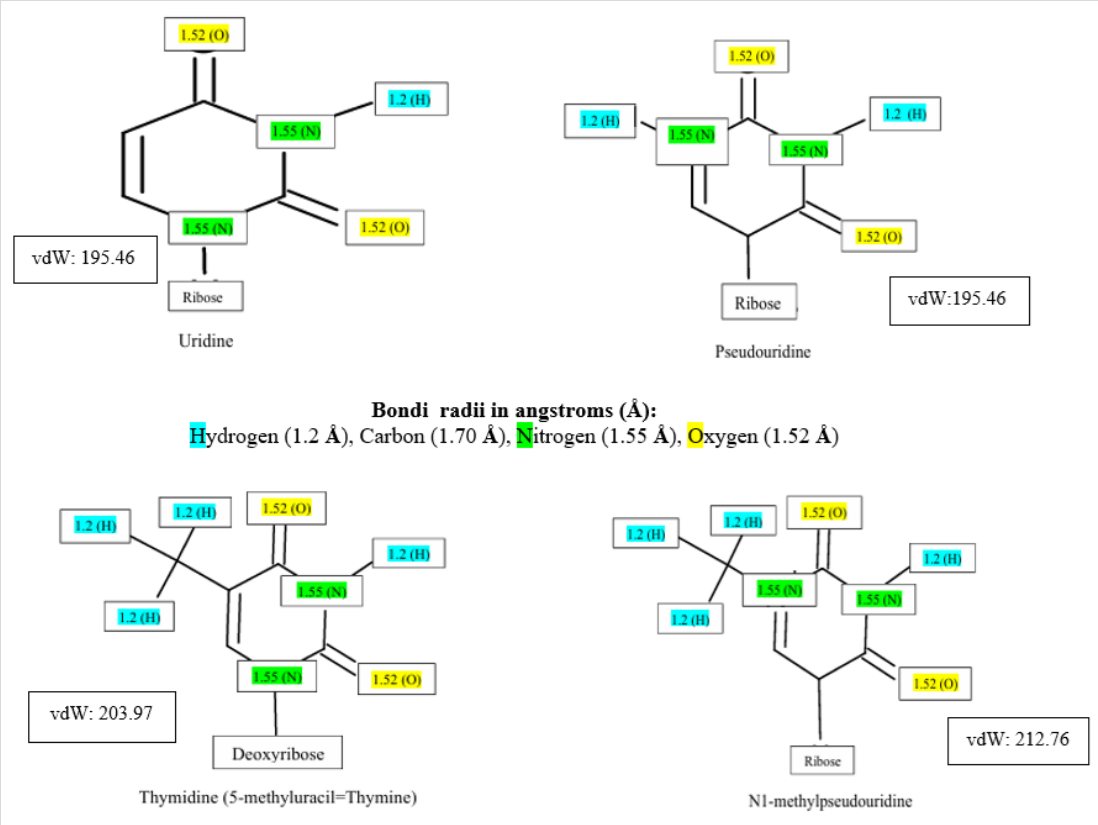

Figure 2: The term Bondi radii specifically refers to the van der Waals radii compiled by A. Bondi in his seminal 1964 paper [73]. These values estimate the effective size of atoms when they are not bonded, essentially, how close two non-bonded atoms can approach each other due to van der Waals forces. Van der Waals value (vdW; from **Table 2**) [51] Bond-line drawings depict the carbon skeleton, the network of carbon atoms forming the molecule's backbone, alongside any attached functional groups, such as CH_3. Lines are drawn in a zigzag pattern so that every vertex and line end represents a carbon atom. Drawn by the author with ChemSketch.

Electronegativity

Adjusting an atom's van der Waals center or its spatial arrangement in a molecule does not alter the electronegativity of an element; that property is determined by its proton count and electron configuration. However, repositioning atoms can:

- Modify bond lengths, bond angles, and overall molecular geometry
- Redistribute electron density across specific regions, affecting local polarity and reactivity. (**see Figure 3**)
- Influence molecular interactions, fold patterns, or recognition systems, without changing intrinsic electronegativity values.

Electronegativity, defined as an atom's tendency to attract shared electrons, and is influenced by chemical environment (e.g., water) [30] and molecular bonding patterns.

To illustrate electronegativity, consider the following analogy:

Water Flow in a Pipe System

- Water = Electrons: Electrons flow or are shared between atoms, like water coursing through pipes.
- Atoms = Pipe Sections: Each bonded atom acts as a pipe segment with specific suction capacity.
- Electronegativity = Suction Power: Highly electronegative atoms (e.g., oxygen, fluorine) behave like segments with strong vacuum pumps, pulling electrons toward themselves.
- Polarity = Flow Distribution: In polar bonds (e.g., H_2O), water pools near stronger pumps (oxygen), creating partial charges (δ^- near oxygen, δ^+ near hydrogen). In nonpolar bonds (e.g., H_2), equal suction allows balanced electron flow.
- Atomic Size = Pipe Diameter: Smaller atoms with higher nuclear charge function like narrower pipe sections, increasing pressure and suction efficiency, i.e., higher electronegativity.

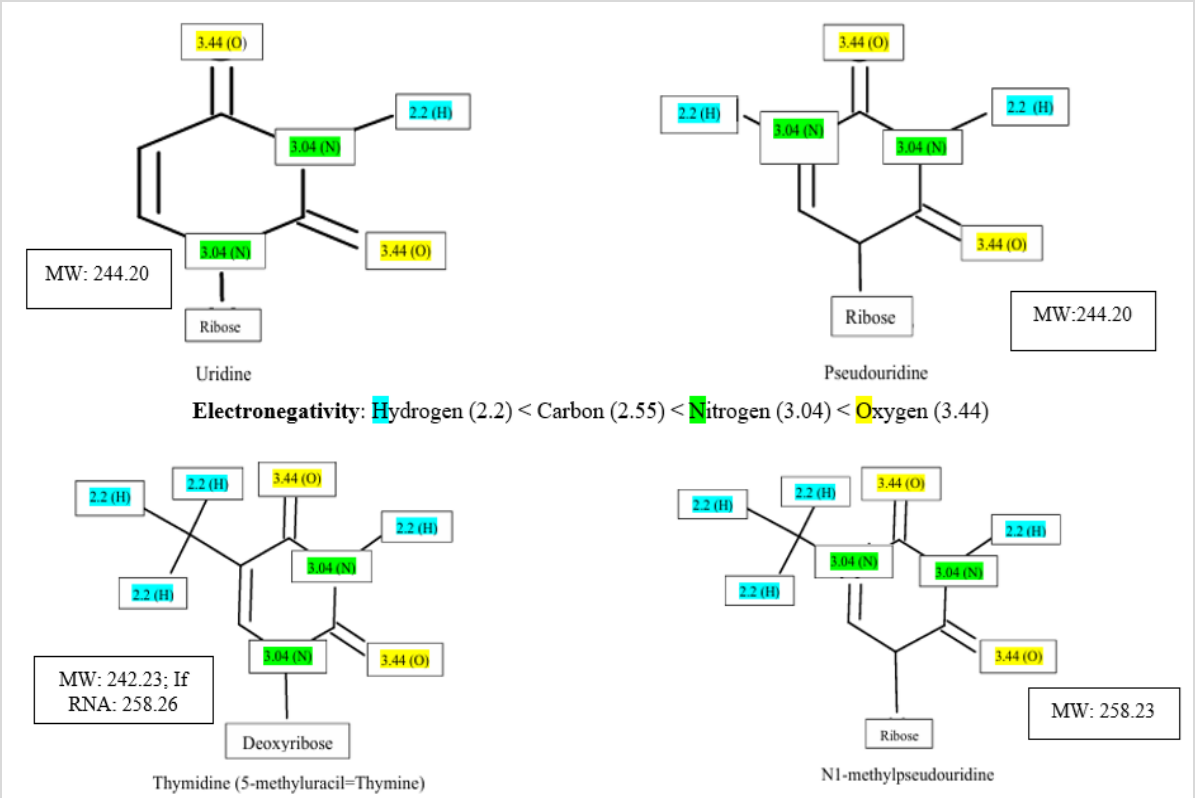

Figure 3: Electronegativity is the tendency of an atom to attract electrons. Influenced by structure, not mass directly. Sum of atomic masses is the molecular weight (g/mol) Heavier atoms often have lower electronegativity. Drawn by the author with ChemSketch.

For example, in the carbonyl (C=O) bond as an example:

- Oxygen (electronegativity 3.44) exerts a strong pull-on electrons.
- Carbon (electronegativity 2.55) exerts a weaker pull.
- The electrons (water) accumulate near oxygen, creating a polar bond with partial charges (δ^- on O, δ^+ on C).

Electronegativity isn't directly calculated for molecular fragments like a carbonyl group (C=O), but its electron-withdrawing effect can be estimated from the individual electronegativities of carbon and oxygen. The dipole moment and partial charges across the C=O bond highlight its ability to attract electron density.

In this analogy, electronegativity, van der Waals dimensions (Bondi radii), and molecular geometry collectively influence RNA base behavior [74,75,76]. Uridine's extensive network of polar bonds functions like a complex pipe system, with multiple vacuum points competing for electron density. By contrast, m1Ψ's thymidine-like profile, presents a more diverse configuration, enhancing π-stacking interactions and lower susceptibility to hydrolysis.

Thymidine like Geometry of m1Ψ

Visual inspection of Table 4 and Figure 2 shows that the three-dimensional shape of m1Ψ most closely parallels thymidine among all standard nucleosides.

Structurally, m1Ψ is derived from pseudouridine via methylation at the N1 position. Its constituent electronegativities, oxygen(3.44), nitrogen(3.04), carbon(2.55), and hydrogen(2.20), remain typical of nucleosides. However, the added methyl group alters the electronic environment of the pseudouridine scaffold.

"This small, monovalent, and lipophilic –CH3 moiety plays a pivotal role in bioactive compounds, influencing both pharmacodynamic and pharmacokinetic profiles [75,76]. Key contributions include:

- Hydrophobic interactions: Displacement of water molecules during molecular recognition enhances binding affinity [75,76].
- Van der Waals participation: The methyl group facilitates subtle, proximity-dependent interactions that stabilize ligand–receptor complexes [75,76].
- Physicochemical modulation: It affects properties such as LogP and aqueous solubility, thereby influencing absorption and distribution [75,76].
- Conformational control: Strategic methylation fine-tunes the three-dimensional architecture of molecular scaffolds, impacting bioactivity and selectivity [75,76]."

From a physicochemical perspective, Bondi radii and electronegativity exhibit an inverse correlation within a given period of the periodic table, each reflecting shifts in nuclear charge and electron cloud distribution. Structural modifications, such as repositioning van der Waals centers or altering glycosidic connectivity (e.g., uridine vs. pseudouridine), do not change elemental electronegativities per se. However, they profoundly reshape molecular geometry, stability, and function by reconfiguring spatial and electronic environments [75,76].

The pseudouracil-ribose backbone of m1Ψ remains intact, affirming its identity as a pseudouridine derivative. Just as pseudouridine's rearranged glycosidic bond differentiates it from uridine, the N1-methyl substitution redistributes electron density enhancing stability and intermolecular interactions [11,47,34,74,75,76].

As summarized in Table 4, m1Ψ's overall geometry aligns more closely to thymidine. Pseudouridine (Ψ) intrinsically stabilizes RNA at the nucleotide level and m1Ψ builds on this stability by further strengthening stacking interactions and reduced hydrolytic reactivity [22,32,47,34,72].

The analogy "If the glove doesn't fit, you must acquit", aptly illustrates how two codons that may encode the same amino acid yet remain chemically and functionally distinct. Although both AUG (adenosine–uridine–guanosine) and its modified counterpart (adenosine–N1-methylpseudouridine–guanosine) are to specify methionine, the substitution alters the mRNA's chemistry, yielding a structurally distinct codon. If the molecular glove doesn't fit perfectly, the consequences extend far beyond superficial similarity.

Conclusion

This paper proposes a quantum perspective that reframes mRNA and DNA stability through the principles of quantum processes, energy conservation, vibrational resonance, and coherence, complementing classical thermodynamics. Existing models emphasize covalent structure, solvent interactions, and entropy but often overlook quantum-scale effects such as tunneling and excitonic coupling. By integrating quantum vibrational and electromagnetic dynamics, predictions of hydrolysis rates and folding stability, particularly in modified nucleic acids, can be refined. I propose a layered thermodynamic architecture in which quantum behaviors enhance the accuracy of classical system predictions. This interdisciplinary framework opens new avenues for designing and testing RNA therapeutics and other biological systems that operate at atomic and molecular scales.

Quantum physics underpins numerous macroscopic chemical properties, including pKa, molecular geometry, and intermolecular forces, by governing electron and nuclear behavior. For example, pKa is determined by electronic structure and solvation, both rooted in quantum phenomena, while atomic masses reflect fundamental nuclear properties. Van der Waals forces, essential for molecular cohesion and biological function, include London dispersion forces arising from quantum fluctuations in electron density, fluctuations permitted by the Heisenberg uncertainty principle. These interactions can be described, at advanced levels, through quantum field theory as exchanges of virtual photons. Molecular geometry, in turn, emerges from probabilistic electron distributions and energy minimization governed by the Schrödinger equation, which defines the spatial characteristics of atomic and molecular orbitals.

To validate the hypotheses flowing from this quantum perspective, future efforts should combine spectroscopy, computational modeling, and synthetic biology to rigorously test and extend these insights

Declarations

Funding Statement

The author received no grant support for this research. It has been funded solely by his own resources and at his own expense.

Conflict of interest

The authors declare that they have no financial or other conflicts of interest with respect to the contents of this article. No external funding was received from any source.

Acknowledgment

Stephanie Seneff, PhD, Senior Research Scientist at the MIT Computer Science and Artificial Intelligence Laboratory (CSAIL), BS biophysics, MS electrical engineering, and PhD computer science, all from MIT, had this to say: "Methyluridine is a known analogue of thymidine; it makes sense that N1-methylpseudouridine would also share properties with thymidine. This arguably makes the mRNA behave a lot more like DNA than like RNA; hence its remarkable stability." I also want to thank my co-editors of the International of Vaccine Theory, Practice, and Research, John Oller, PhD, for reviewing the details of the accompanying tables and figures in this paper. I must include in that list Mary Holland, MA, JD, James Lyons-Weiler, PhD, Daniel Broudy, PhD, and Ulrike Granögger of the Solari Report with Catherine Austin Fitts (former US cabinet member). Any remaining errors or infelicities are my own.

References

[1] Alberts, B., Johnson, A., Lewis, J., Raff, M., Roberts, K., & Walter, P. (2002). Molecular biology of the cell (4th ed.). Garland Science.

[2] Berg, J. M., Tymoczko, J. L., Gatto, G. J., & Stryer, L. (2015). Biochemistry (8th ed.). W. H. Freeman.

[3] Yu, Z., & Cowan, J. A. (1999). Human DNA repair systems: An overview. Environmental and Molecular Mutagenesis, 33(1), 3–20. https://doi.org/10.1002/(sici)1098-2280(1999)33:1<3::aid-em2>3.0.co;2-l

[4] Santiago, D. (2025). A quantum timing change: Codon energetics [Preprint]. https://doi.org/10.20944/preprints202503.0548.v2

[5] Lambert, N., Chen, Y.-N., Cheng, Y.-C., Li, C.-M., Chen, G.-Y., & Nori, F. (2013). Quantum biology. Nature Physics, 9(1), 10–18. https://doi.org/10.1038/nphys2474

[6] Bohm, D. (1980). Wholeness and the implicate order. Routledge.

[7] Engel, G. S., Calhoun, T. R., Read, E. L., Ahn, T.-K., Mancal, T., Cheng, Y.-C., Blankenship, R. E., & Fleming, G. R. (2007). Evidence for wavelike energy transfer through quantum coherence in photosynthetic systems. Nature, 446(7137), 782–786. https://doi.org/10.1038/nature05678

[8] Peirce, C. S. (1863). The chemical theory of interpenetration. American Journal of Science, s2-35(103), 78–82. https://doi.org/10.2475/ajs.s2-35.103.78

[9] Fenter, P., & Lee, S. S. (2014). Hydration layer structure at solid–water interfaces. MRS Bulletin, 39(12), 1056–1061. https://doi.org/10.1557/mrs.2014.252

[10] Pietruszka, M., & Marzec, M. (2024). Ultra-weak photon emission from DNA. Scientific reports, 14(1), 28915. https://doi.org/10.1038/s41598-024-80469-0

[11] Santiago, D. (2024). A Closer Look at N1-methylpseudouridine in the modified mRNA injectables. International Journal of Vaccine Theory, Practice, and Research, 3(2), 1345–1366. https://doi.org/10.56098/5azda593

[12] Klinman, J. P., & Kohen, A. (2013). Hydrogen tunneling links protein dynamics to enzyme catalysis. Annual Review of Biochemistry, 82, 471–496. https://doi.org/10.1146/annurev-biochem-051710-133623

[13] González-Jiménez, M., Ramakrishnan, G., Tukachev, N. V., Senn, H. M., & Wynne, K. (2021). Low-frequency vibrational modes in G-quadruplexes reveal the mechanical properties of nucleic acids. Physical Chemistry Chemical Physics, 23(23), 13250–13260. https://doi.org/10.1039/D0CP05404F

[14] Jiang, Y., & Wang, L. (2019). Development of Vibrational Frequency Maps for Nucleobases. The journal of physical chemistry. B, 123(27), 5791–5804. https://doi.org/10.1021/acs.jpcb.9b04633

[15] Bothma, J. P., Gilmore, J. B., & McKenzie, R. H. (2010). The role of quantum effects in proton transfer reactions in enzymes: Quantum tunneling in a noisy environment? New Journal of Physics, 12(5), Article 055002. https://doi.org/10.1088/1367-2630/12/5/055002

[16] Bruening, E. M., Schauss, J., Siebert, T., Fingerhut, B. P., & Elsaesser, T. (2018). Vibrational Dynamics and Couplings of the Hydrated RNA Backbone: A Two-Dimensional Infrared Study. The Journal of Physical Chemistry Letters, 9(3), 583–587. https://doi.org/10.1021/acs.jpclett.7b03314

[17] Heidari, A. (2016). An analytical and computational infrared spectroscopic review of vibrational modes in nucleic acids. Austin Journal of Analytical and Pharmaceutical Chemistry, 3(1), Article 1058.

[18] Owens, A., Support, S. A., & IDT. (n.d.). Unraveling RNA: The importance of a 2' hydroxyl | IDT. Integrated DNA Technologies. Retrieved July 13, 2025, from https://www.idtdna.com/pages/education/decoded/article/unraveling-rna-the-importance-of-a-2-hydroxyl

[19] Jiang, Y., & Wang, L. (2020). Modeling the vibrational couplings of nucleobases. The Journal of chemical physics, 152(8), 084114. https://doi.org/10.1063/1.5141858 (Zambito, L. Research. Wang Research Group, Department of Chemistry and Chemical Biology | Rutgers, The State University of New Jersey. Retrieved July 11, 2025, from https://wanggroup.rutgers.edu/research)

[20] Peng, C. S., Jones, K. C., & Tokmakoff, A. (2011). Anharmonic vibrational modes of nucleic acid bases revealed by 2D IR spectroscopy. Journal of the American Chemical Society, 133(39), 15650–15660. https://doi.org/10.1021/ja205636h

[21] Aamouche, A., Ghomi, M., Letellier, R., Liquier, J., Morvan, F., Cadet, J., & Taillandier, E. (1995). Neutron inelastic scattering, optical spectroscopies and scaled quantum mechanical force fields for analysing the vibrational dynamics of pyrimidine nucleic acid bases: Uracil, thymine and cytosine. In J. C. Merlin, S. Turrell, & J. P. Huvenne (Eds.), Spectroscopy of biological molecules (pp. 493–494). Springer. https://doi.org/10.1007/978-94-011-0371-8_139

[22] Parr, C. J. C., Wada, S., Kotake, K., Kameda, S., Matsuura, S., Sakashita, S., Park, S., Sugiyama, H., Kuang, Y., & Saito, H. (2020). N1-methylpseudouridine substitution enhances the performance of synthetic mRNA switches in cells. Nucleic Acids Research, 48(6), Article e35. https://doi.org/10.1093/nar/gkaa070

[23] Nance, K. D., & Meier, J. L. (2021). Modifications in an emergency: The role of N1-methylpseudouridine in COVID-19 vaccines. ACS Central Science, 7(5), 748–756. https://doi.org/10.1021/acscentsci.1c00197

[24] Finol, E., Krul, S. E., Hoehn, S. J., Lyu, X., & Crespo-Hernández, C. E. (2024). The mRNACalc webserver accounts for the N1-methylpseudouridine hypochromicity to enable precise nucleoside-modified mRNA quantification. Molecular therapy. Nucleic acids, 35(2), 102171. https://doi.org/10.1016/j.omtn.2024.102171

[25] Morais, P., Adachi, H., & Yu, Y.-T. (2021). The Critical Contribution of Pseudouridine to mRNA COVID-19 Vaccines. Frontiers in Cell and Developmental Biology, 9. https://doi.org/10.3389/fcell.2021.789427

[26] Kim, Y., Bertagna, F., D'Souza, E. M., Heyes, D. J., Johannissen, L. O., Nery, E. T., Pantelias, A., Sanchez-Pedreño Jimenez, A., Slocombe, L., Spencer, M. G., Al-Khalili, J., Engel, G. S., Hay, S., Hingley-Wilson, S. M., Jeevaratnam, K., Jones, A. R., Kattnig, D. R., Lewis, R., Sacchi, M., ... McFadden, J. (2021). Quantum Biology: An Update and Perspective. Quantum Reports, 3(1), 80-126. https://doi.org/10.3390/quantum3010006

[27] Kurian, P., Dunston, G., & Lindesay, J. (2016). How quantum entanglement in DNA synchronizes double-strand breakage by type II restriction endonucleases. Journal of theoretical biology, 391, 102–112. https://doi.org/10.1016/j.jtbi.2015.11.018

[28] Manzano, Daniel (2020). "A short introduction to the Lindblad master equation". AIP Advances. 10 (2): 025106. arXiv:1906.04478. Bibcode:2020AIPA...10b5106M. doi:10.1063/1.5115323. S2CID 184487806.

[29] Lindblad, G. On the generators of quantum dynamical semigroups. Commun. Math. Phys. 48, 119–130 (1976). https://doi.org/10.1007/BF01608499

[30] Pollack, G. H. (2013). The fourth phase of water: Beyond solid, liquid, and vapor. Ebner & Sons.

[31] Andries, O., Mc Cafferty, S., De Smedt, S. C., Weiss, R., Sanders, N. N., & Kitada, T. (2015). N[1]-methylpseudouridine-incorporated mRNA outperforms

pseudouridine-incorporated mRNA by providing enhanced protein expression and reduced immunogenicity in mammalian cell lines and mice. Journal of Controlled Release, 217, 337–344. https://doi.org/10.1016/j.jconrel.2015.08.051

[32] Chen, S., Liu, Z., Cai, J., Li, H., & Qiu, M. (2024). N1-methylpseudouridine modification level correlates with protein expression, immunogenicity, and stability of mRNA. MedComm, 5(9), Article e691. https://doi.org/10.1002/mco2.691

[33] Bhattacharjee, B., Lu, P., Monteiro, V. S., Tabachnikova, A., Wang, K., Hooper, W. B., Bastos, V., Greene, K., Sawano, M., Guirgis, C., Tzeng, T. J., Warner, F., Baevova, P., Kamath, K., Reifert, J., Hertz, D., Dressen, B., Tabacof, L., Wood, J., … Iwasaki, A. (2025). Immunological and Antigenic Signatures Associated with Chronic Illnesses after COVID-19 Vaccination (p. 2025.02.18.25322379). medRxiv. https://doi.org/10.1101/2025.02.18.25322379

[34] Kierzek, E., Malgowska, M., Lisowiec, J., Turner, D. H., Gdaniec, Z., & Kierzek, R. (2014). The contribution of pseudouridine to stabilities and structure of RNAs. Nucleic acids research, 42(5), 3492–3501. https://doi.org/10.1093/nar/gkt1330

[35] Schnappinger, T., Falvo, C., & Kowalewski, M. (2024). Disentangling collective coupling in vibrational polaritons with double quantum coherence spectroscopy. The Journal of Chemical Physics, 161(24), 244107. https://doi.org/10.1063/5.0239877

[36] Davis D. R. (1995). Stabilization of RNA stacking by pseudouridine. Nucleic acids research, 23(24), 5020–5026. https://doi.org/10.1093/nar/23.24.5020

[37] Jalilvand, S., & Mousavi, H. (2024). Vibration spectra of DNA and RNA segments. European Biophysics Journal, 53, 95–109. https://doi.org/10.1007/s00249-023-01699-0

[38] Mulroney, T. E., Pöyry, T., Yam-Puc, J. C., Rust, M., Harvey, R. F., Kalmar, L., Horner, E., Booth, L., Ferreira, A. P., Stoneley, M., Sawarkar, R., Mentzer, A. J., Lilley, K. S., Smales, C. M., von der Haar, T., Turtle, L., Dunachie, S., Klenerman, P., Thaventhiran, J. E. D., & Willis, A. E. (2024). N1-methylpseudouridylation of mRNA causes +1 ribosomal frameshifting. Nature, 625(7993), 189–194. https://doi.org/10.1038/s41586-023-06800-3

[39] Adam, J., Adamczyk, L., Adams, J. R., Adkins, J. K., Agakishiev, G., Aggarwal, M. M., Ahammed, Z., Alekseev, I., Anderson, D. M., Aparin, A., Aschenauer, E. C., Ashraf, M. U., Atetalla, F. G., Attri, A., Averichev, G. S., Bairathi, V., Barish, K., Behera, A., Bellwied, R., … Zyzak, M. (2021). Measurement of e^+e^- Momentum and Angular Distributions from Linearly Polarized Photon Collisions. Phys. Rev. Lett., 127(5), 052302. https://doi.org/10.1103/PhysRevLett.127.052302

[40] He, X., Gong, Y., Xie, F., Wang, Y., Dong, D., Li, Y., & Zhang, Z. (2023). RNA degformer: accurate prediction of mRNA degradation at nucleotide resolution with deep learning. Briefings in Bioinformatics, 24(1), bbac581. https://doi.org/10.1093/bib/bbac581

[41] Irrgang, P., Gerling, J., Kocher, K., Lapuente, D., Steininger, P., Habenicht, K., Wytopil, M., Beileke, S., Schäfer, S., Zhong, J., Ssebyatika, G., Krey, T., Falcone, V., Schülein, C., Peter, A. S., Nganou-Makamdop, K., Hengel, H., Held, J., Bogdan, C., Überla, K., … Tenbusch, M. (2023). Class switch toward noninflammatory, spike-specific IgG4 antibodies after repeated SARS-CoV-2 mRNA vaccination. Science immunology, 8(79), eade2798. https://doi.org/10.1126/sciimmunol.ade2798

[42] Valk, A. M., Keijser, J. B. D., van Dam, K. P. J., Stalman, E. W., Wieske, L., Steenhuis, M., Kummer, L. Y. L., Spuls, P. I., Bekkenk, M. W., Musters, A. H., Post, N. F., Bosma, A. L., Horváth, B., Hijnen, D. J., Schreurs, C. R. G., van Kempen, Z. L. E., Killestein, J., Volkers, A. G., Tas, S. W., Boekel, L., … T2B! Immunity against SARS-CoV-2 study group (2024). Suppressed IgG4 class switching in dupilumab- and TNF inhibitor-treated patients after mRNA vaccination. Allergy, 79(7), 1952–1961. https://doi.org/10.1111/all.16089

[43] Brogna, C., Cristoni, S., Marino, G., Montano, L., Viduto, V., Fabrowski, M., Lettieri, G., & Piscopo, M. (2023). Detection of recombinant Spike protein in the blood of individuals vaccinated against SARS-CoV-2: Possible molecular mechanisms. Proteomics. Clinical applications, e2300048. Advance online publication. https://doi.org/10.1002/prca.202300048

[44] Bansal, S., Perincheri, S., Fleming, T., Poulson, C., Tiffany, B., Bremner, R. M., & Mohanakumar, T. (2021). Cutting Edge: Circulating Exosomes with COVID Spike Protein Are Induced by BNT162b2 (Pfizer-BioNTech) Vaccination prior to Development of Antibodies: A Novel Mechanism for Immune Activation by mRNA Vaccines. Journal of immunology (Baltimore, Md.: 1950), 207(10), 2405–2410. https://doi.org/10.4049/jimmunol.2100637

[45] Kim, S. C., Sekhon, S. S., Shin, W.-R., Ahn, G., Cho, B.-K., Ahn, J.-Y., & Kim, Y.-H. (2022). Modifications of mRNA vaccine structural elements for improving mRNA stability and translation efficiency. Molecular & Cellular Toxicology, 18(1), 1–8. https://doi.org/10.1007/s13273-021-00171-4

[46] Monroe, J., Eyler, D. E., Mitchell, L., Deb, I., Bojanowski, A., Srinivas, P., Dunham, C. M., Roy, B., Frank, A. T., & Koutmou, K. S. (2024). N1-Methylpseudouridine and pseudouridine modifications modulate mRNA decoding during translation. Nature communications, 15(1), 8119. https://doi.org/10.1038/s41467-024-51301-0

[47] Dutta, N., Deb, I., Sarzynska, J., & Lahiri, A. (2023). Structural and thermodynamic consequences of base pairs containing pseudouridine and N1-methylpseudouridine in RNA duplexes. bioRxiv, 2023.03.19.533340. https://doi.org/10.1101/2023.03.19.533340

[48] Riback JA, Eeftens JM, Lee DSW, Quinodoz SA, Donlic A, Orlovsky N, Wiesner L, Beckers L, Becker LA, Strom AR, Rana U, Tolbert M, Purse BW, Kleiner R, Kriwacki R, Brangwynne CP. Viscoelasticity and advective flow of RNA underlies nucleolar form and function. Mol Cell. 2023 Sep 7;83(17):3095-3107.e9. doi: 10.1016/j.molcel.2023.08.006. PMID: 37683610; PMCID: PMC11089468.

[49] Balani, K., Verma, V., Agarwal, A., & Narayan, R.J. (2015). Physical, Thermal, and Mechanical Properties of Polymers. doi:10.1002/9781118950623.APP1 https://api.semanticscholar.org/CorpusID:136705313

[50] Roe, B.A. & Tsen, H.Y. (1977). Role of Ribothymidine in Mammalian tRNAPhe. Proceedings of the National Academy of Sciences USA, 74(9), 3696–3700.

[51] Zhao, Y. H., Abraham, M. H., & Zissimos, A. M. (2003). Fast Calculation of van der Waals Volume as a Sum of Atomic and Bond Contributions and Its Application to

Drug Compounds. The Journal of Organic Chemistry, 68(19), 7368–7373. https://doi.org/10.1021/jo034808o

[52] Jones, E. L., Mlotkowski, A. J., Hebert, S. P., Schlegel, H. B., & Chow, C. S. (2022). Calculations of pKa Values for a Series of Naturally Occurring Modified Nucleobases. The Journal of Physical Chemistry A, 126(9), 1518–1529. https://doi.org/10.1021/acs.jpca.1c10905

[53] National Center for Biotechnology Information (2025). PubChem Compound Summary for CID 99543, N1-Methylpseudouridine. Retrieved July 21, 2025 from https://pubchem.ncbi.nlm.nih.gov/compound/N1-Methylpseudouridine.

[54] Hermann, J., & Tkatchenko, A. (2020). Density Functional Model for van der Waals Interactions: Unifying Many-Body Atomic Approaches with Nonlocal Functionals. Physical review letters, 124(14), 146401. https://doi.org/10.1103/PhysRevLett.124.146401

[55] Seneff, S., Nigh, G., Kyriakopoulos, A. M., & McCullough, P. A. (2022). Innate immune suppression by SARS-CoV-2 mRNA vaccinations: The role of G-quadruplexes, exosomes, and MicroRNAs. Food and Chemical Toxicology, 164, 113008. https://doi.org/10.1016/j.fct.2022.113008

[56] Demongeot, J.; Fougère, C. mRNA COVID-19 Vaccines—Facts and Hypotheses on Fragmentation and Encapsulation. Vaccines 2023, 11, 40. https://doi.org/10.3390/ vaccines11010040

[57] Press release: The Nobel Prize in Chemistry 2024. (n.d.). NobelPrize.Org. Retrieved July 24, 2025, from https://www.nobelprize.org/prizes/chemistry/2024/press-release/

[58] Brookes, J. C. (2017). Quantum effects in biology: golden rule in enzymes, olfaction, photosynthesis and magnetodetection. Proceedings. Mathematical, physical, and engineering sciences, 473(2201), 20160822. https://doi.org/10.1098/rspa.2016.0822

[59] Celebi Torabfam, G., K Demir, G., & Demir, D. (2023). Quantum tunneling time delay investigation of KK+ ion in human telomeric G-quadruplex systems. Journal of biological inorganic chemistry : JBIC: a publication of the Society of Biological Inorganic Chemistry, 28(2), 213–224. https://doi.org/10.1007/s00775-022-01982-z

[60] McKernan, K., Kyriakopoulos, A. M., & McCullough, P. A. (2021, November 25). Differences in Vaccine and SARS-CoV-2 Replication Derived mRNA: Implications for Cell Biology and Future Disease. https://doi.org/10.31219/osf.io/bcsa6 McKernan, K., Kyriakopoulos, A. M., & McCullough, P. A. (2021, November 25). Differences in Vaccine and SARS-CoV-2 Replication Derived mRNA: Implications for Cell Biology and Future Disease. https://doi.org/10.31219/osf.io/bcsa6

[61] Bhattacharyya, D., Mirihana Arachchilage, G., & Basu, S. (2016). Metal Cations in G-Quadruplex Folding and Stability. Front. Chem., 4, 38. https://doi.org/10.3389/fchem.2016.00038

[62] Wang, Y.-T., Tang, J.-S., Wei, Z.-Y., Yu, S., Ke, Z.-J., Xu, X.-Y., Li, C.-F., & Guo, G.-C. (2017). Directly Measuring the Degree of Quantum Coherence using Interference Fringes. Phys. Rev. Lett., 118(2), 020403. https://doi.org/10.1103/PhysRevLett.118.020403

[63] Geesink, H., Jerman, I., & Meijer, D. K. F. (2020). The cradle of life: WATER via its coherent quantum frequencies. WATER Journal, 11, Article 1. https://doi.org/10.14294/water.2020.1

[64] Montagnier, L., Del Giudice, E., Aïssa, J., Lavallee, C., Motschwiller, S., Capolupo, A., … Vitiello, G. (2015). Transduction of DNA information through water and electromagnetic waves. Electromagnetic Biology and Medicine, 34(2), 106–112. https://doi.org/10.3109/15368378.2015.1036072

[65] Ho, L. L. Y., Schiess, G. H. A., Miranda, P., Weber, G., & Astakhova, K. (2024). Pseudouridine and N1-methylpseudouridine as potent nucleotide analogues for RNA therapy and vaccine development. RSC Chem. Biol., 5(5), 418–425. https://doi.org/10.1039/D4CB00022F

[66] Winkler, M., Giuliano, B. M., & Caselli, P. (2020). UV Resistance of Nucleosides: An Experimental Approach. ACS Earth and Space Chemistry, 4(11), 2320–2326. https://doi.org/10.1021/acsearthspacechem.0c00228

[67] Cavaluzzi, M. J., & Borer, P. N. (2004). Revised UV extinction coefficients for nucleoside-5′-monophosphates and unpaired DNA and RNA. Nucleic Acids Research, 32(1), e13. https://doi.org/10.1093/nar/gnh015

[68] Lai, H. & Levitt, B. (2024). Cellular and molecular effects of non-ionizing electromagnetic fields. Reviews on Environmental Health, 39(3), 519-529. https://doi.org/10.1515/reveh-2023-0023

[69] Sun, G., Li, J., Zhou, W., Hoyle, R. G., & Zhao, Y. (2022). Electromagnetic interactions in regulations of cell behaviors and morphogenesis. Front. Cell Dev. Biol., 10, 1014030. https://doi.org/10.3389/fcell.2022.1014030

[70] Perez, F. P., Bandeira, J. P., Perez Chumbiauca, C. N., Lahiri, D. K., Morisaki, J., & Rizkalla, M. (2022). Multidimensional insights into the repeated electromagnetic field stimulation and biosystems interaction in aging and age-related diseases. Journal of Biomedical Science, 29(1), 39. https://doi.org/10.1186/s12929-022-00825-y

[71] Bittner, E. R., Madalan, A., Czader, A., & Roman, G. (2012). Quantum origins of molecular recognition and olfaction in drosophila. The Journal of Chemical Physics, 137(22), 22A551. https://doi.org/10.1063/1.4767067

[72] Zefirov, Y. V., & Zorkii, P. M. (1989). Van der Waals radii and their application in chemistry. Russian Chemical Reviews, 58(5), 421. https://doi.org/10.1070/RC1989v058n05ABEH003451

[73] Bondi, A. (1964). Van der Waals Volumes and Radii. The Journal of Physical Chemistry, 68(3), 441–451. https://doi.org/10.1021/j100785a001

[74] Wolken, J. K., & Ture ek, F. (2000). Proton affinity of uracil. A computational study of protonation sites. Journal of the American Society for Mass Spectrometry, 11(12), 1065–1071. https://doi.org/10.1016/s1044-0305(00)00176-8

[75] Pinheiro PSM, Franco LS, Fraga CAM. The Magic Methyl and Its Tricks in Drug Discovery and Development. Pharmaceuticals (Basel). 2023 Aug 15;16(8):1157. doi: 10.3390/ph16081157. PMID: 37631072; PMCID: PMC10457765.

[76] Barreiro EJ, Kümmerle AE, Fraga CA. The methylation effect in medicinal chemistry. Chem Rev. 2011 Sep 14;111(9):5215-46. doi: 10.1021/cr200060g. Epub 2011 Jun 1. PMID: 21631125.

Notes [51]

To calculate the van der Waals volume (VdW) for uridine using the Atomic and Bond Contributions (VABC) method from the paper, follow these steps. The method is based on Bondi atomic radii and approximates VvdW in Å³/molecule. It requires only the molecular formula, atom types, number of bonds, and ring counts, no specialized software is needed. The formula is:

VdW = ∑ (all atom contributions) - 5.92 × NB - 14.7 × RA - 3.8 × RNR, Where:

- ∑ (all atom contributions) is the sum of individual atomic van der Waals volumes (from Table 2 in the paper).
- NB is the total number of bonds (count each bond as one, regardless of whether it is single, double, or triple).
- RA is the number of aromatic rings.
- RNR is the number of nonaromatic rings (labeled RNA in the paper).

NB can be calculated using the simplified algorithm: NB = N - 1 + RA + RNR (where N is the total number of atoms).

Method and Potential Variations

- This is an approximation validated in the paper against computer programs (e.g., TSAR, MacroModel) for 677 organic compounds, including drugs. For uridine (a drug-like compound), it should be reliable, with typical errors around 1-2% based on the paper's standard deviations.
- If converting to cm³/mol, multiply by 0.602 (Avogadro's number factor, as noted in the paper).
- The method assumes standard Bondi radii and ignores conformational details or solvent effects; it's for intrinsic molecular volume.
- For verification, you can implement this in a spreadsheet (as suggested in the paper) or compare to computational tools like TSAR (which correlates via VdW(TSAR) ≈ 0.801 × VdW (VABC) + 0.18).

The van der Waals volume (VdW) for N1-methylpseudouridine is calculated using the Atomic and Bond Contributions (VABC) method as described in the outline, adapted from uridine to account for the additional methyl group at N1.

1. Determine the molecular formula: $C_{10}H_{14}N_2O_6$.
2. Total number of atoms (N): 10 C + 14 H + 2 N + 6 O = 32.
3. Number of aromatic rings (RA): 1 (pyrimidine ring in the base).
4. Number of nonaromatic rings (RNR): 1 (furanose ring in the ribose).
5. Total number of bonds (NB): N - 1 + RA + RNR = 32 - 1 + 1 + 1 = 33.
6. Sum of individual atomic van der Waals volumes (from Bondi radii, as the basis for Table 2 in the paper):

C: 20.58 Å³ each → 10 × 20.58 = 205.8 Å³
H: 7.24 Å³ each → 14 × 7.24 = 101.36 Å³
N: 15.60 Å³ each → 2 × 15.60 = 31.2 Å³
O: 14.71 Å³ each → 6 × 14.71 = 88.26 Å³
Total sum: 205.8 + 101.36 + 31.2 + 88.26 = 426.62 Å³

7. Calculate VdW: sum - 5.92 × NB - 14.7 × RA - 3.8 × RNR = 426.62 - 5.92 × 33 - 14.7 × 1 - 3.8 × 1 = 426.62 - 195.36 - 14.7 - 3.8 = 212.76 Å³/molecule.

The atomic volumes are derived from Bondi radii (r_C = 1.7 Å, r_H = 1.2 Å, r_N = 1.55 Å, r_O = 1.52 Å) using $V = (4/3)\pi r^3$. The method approximates VvdW with typical errors of 1-2%.